The changing structural chemistry of lithium anilide on solvation by pyridine, 4-methylpyridine or 4-*tert*-butylpyridine

William Clegg,[a] Lynne Horsburgh,[a] Stephen T. Liddle,[a] Fiona M. Mackenzie,[b] Robert E. Mulvey *[b] and Alan Robertson[b]

[a] *Department of Chemistry, University of Newcastle, Newcastle-upon-Tyne, UK NE1 7RU*
[b] *Department of Pure and Applied Chemistry, University of Strathclyde, Glasgow, UK G1 1XL.*
   E-mail: R.E.Mulvey@strath.ac.uk

A family of crystalline lithium anilide solvates, $[\{PhN(H)Li\cdot(pyr)_2\}_2]$ **1**, $[\{PhN(H)Li\cdot(4\text{-}Me\text{-}pyr)_2\}_2]$ **2** and $[\{PhN(H)Li\}_4\cdot(4\text{-}Bu^t\text{-}pyr)_6]$ **3** has been synthesised by reacting the aromatic primary amide with two molar equivalents of the appropriate pyridine-based solvent (pyridine, 4-methylpyridine and 4-*tert*-butylpyridine, respectively) in hexane–toluene solution. X-Ray crystallographic studies have revealed three contrasting structures: **1** adopts a dinuclear, dimeric $[(anilido)N\text{–}Li]_2$ ring arrangement with a transoid (*anti*) conformation of amido substituents; **2** adopts a similar arrangement but with a cisoid (*syn*) conformation of amido substituents; and **3** adopts a novel tetranuclear arrangement with a central $[(anilido)N\text{–}Li]_2$ transoid ring, separating two mixed ligand $[(anilido)N\text{–}Li\text{-}(pyr)N\text{–}Li]$ rings, made possible by the unusual μ-bonding of a 4-*tert*-butylpyridine ligand. A combination of ^1H, ^7Li and ^{13}C NMR spectroscopic studies at 300 K suggests similar environments exist for corresponding atoms in $[^2H_8]$-toluene solutions of **1**, **2** or **3**. Further examination of the solution of **3** over the temperature window (300–193 K) has detected a fluxional structure involving the intramolecular exchange of two distinct types of anilido ligand, consistent with those present in the molecular structure of crystalline **3**.

Introduction

Long overshadowed by their illustrious secondary counterparts, the synthetic applications of which are legion,[1] lithiated primary amines [RN(H)Li] are themselves now emerging as important and versatile chemical reagents. Their distinguishing formulaic feature, the hydrogen atom attached to nitrogen, has a dichotomous role in this utility: on the one hand, it limits the steric bulk of the amido anion and so renders them less effective than secondary amides such as lithium diisopropylamide or lithium hexamethyldisilazide in the art of proton abstraction; on the other hand, its removal opens a gateway to organoimido (RN^{2-}) chemistry, which is burgeoning as a consequence. Thus, whilst still largely unused by the synthetic organic community,[2] lithium primary amides are being increasingly utilised by inorganic and organometallic chemists. This has resulted in the discovery of many interesting new chemical species of which heterobimetallic $[\{(MesNH)Sn(Nma)\}_2(Li\cdot 2THF)_2]$ (Mes = 2,4,6-Me$_3$C$_6$H$_2$; ma = 2-MeOC$_6$H$_4$),[3] heterotrimetallic $[\{[PhN(H)]_2(Bu^tO)LiNaK\cdot(TMEDA)_2\}_2]$,[4] and the triazasulfite anion $[S(NBu^t)_3]^{2-}$,[5] are representative recent examples. The structural chemistry of lithium primary amides is developing in step with their chemical utilisation. Such information on the nature of these "building blocks" is essential when endeavouring to synthesise particular heterometallic complexes by a rational *aufbau* approach. On a more fundamental level, this knowledge also enables comparison and contrast with the vast library of data available on their secondary counterparts.[6] In this regard, it is significant that the belated crystallographic confirmation of a polymeric ladder arrangement, long postulated to exist, was established not through a secondary amide structure, but through the two primary amide structures of the ethylenediamide $[\{H_2NCH_2CH_2N(H)Li\}_\infty]$[7] and the monobenzylamide $[\{[PhCH_2N(H)Li]_2\cdot H_2NCH_2Ph\}_\infty]$.[8]

Insight into how such an infinite ladder might disassemble in a stepwise manner to ultimately release a more reactive oligomer has also come from recent studies of lithium primary amide structures.[9,10] Implicit in this work is the idea that even apparently "simple" amides can have a complicated, challenging structural chemistry, dependent not only on the coordinating solvent present but also on solvent concentration. Thus the simplest aromatic amide, lithium anilide can, when made in the presence of different concentrations of THF, crystallize in two radically distinct structural forms: hexanuclear $[\{PhN(H)Li\}_6\cdot 8THF]$[11] and dinuclear $[\{PhN(H)Li\cdot(THF)_2\}_2]$.[12] Changing the solvent ligand to tridentate PMDETA $[N,N,N',N'',N''$-pentamethyldiethylenetriamine, $(Me_2NCH_2CH_2)_2NMe]$ also throws up a surprise in trinuclear $[\{PhN(H)Li\}_3\cdot PMDETA]$,[13] notable for its simultaneous exhibition of three-, four- and five-coordinate lithium atoms. Given that the solvent can exert such a dramatic structural influence, we have been examining systematically the effects that other coordinating solvents can have on the appearance of lithium anilide. Here, in this paper, we report on the structures obtained when lithium anilide is solvated by a series of pyridine-based solvents, namely, in order of increasing steric bulk, pyridine (pyr), 4-methylpyridine (4-Me-pyr) or 4-*tert*-butylpyridine (4-Bu^t-pyr). Interestingly, significant variations are observed despite the fact that the substitutional differences between the pyridines (H, Me, ^{t}Bu, respectively) occur at the γ-position, furthermost from the ligating N centre.
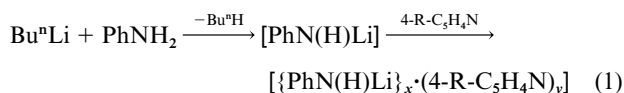
Results and discussion

Syntheses

Three new solid-state lithium anilide solvates have been prepared during the course of this study: $[\{PhN(H)Li\cdot(pyr)_2\}_2]$ (**1**),

Table 1 Selected bond lengths (Å) and angles (°) for **1**

Li(1)–N(1)	2.018(7)	Li(1)–N(2)	2.005(6)
Li(2)–N(1)	2.016(7)	Li(2)–N(2)	2.046(7)
Li(1)–N(3)	2.067(7)	Li(1)–N(6)	2.087(7)
Li(2)–N(4)	2.105(7)	Li(2)–N(5)	2.076(7)
N(1)–C(1)	1.385(5)	N(2)–C(7)	1.367(4)
N(3)–C(13)	1.340(5)	N(3)–C(17)	1.330(5)
N(4)–C(18)	1.293(5)	N(4)–C(22)	1.314(5)
N(5)–C(23)	1.324(5)	N(5)–C(27)	1.322(5)
N(6)–C(28)	1.339(5)	N(6)–C(32)	1.337(5)
N(2)–Li(1)–N(1)	103.6(3)	N(2)–Li(1)–N(3)	111.4(3)
N(1)–Li(1)–N(3)	123.6(3)	N(2)–Li(1)–N(6)	118.2(3)
N(1)–Li(1)–N(6)	101.0(3)	N(3)–Li(1)–N(6)	99.6(3)
N(1)–Li(2)–N(2)	102.2(3)	N(1)–Li(2)–N(5)	122.9(3)
N(2)–Li(2)–N(5)	107.9(3)	N(1)–Li(2)–N(4)	103.8(3)
N(2)–Li(2)–N(4)	121.2(3)	N(5)–Li(2)–N(4)	100.3(3)
C(1)–N(1)–Li(2)	131.3(3)	C(1)–N(1)–Li(1)	132.5(4)
Li(2)–N(1)–Li(1)	77.2(3)	C(7)–N(2)–Li(1)	132.7(3)
C(7)–N(2)–Li(2)	115.8(3)	Li(1)–N(2)–Li(2)	76.8(3)
C(17)–N(3)–C(13)	116.4(4)	C(17)–N(3)–Li(1)	117.4(3)
C(13)–N(3)–Li(1)	126.1(3)	C(18)–N(4)–C(22)	114.6(4)
C(18)–N(4)–Li(2)	125.0(3)	C(22)–N(4)–Li(2)	120.3(3)
C(27)–N(5)–C(23)	116.8(3)	C(27)–N(5)–Li(2)	124.1(3)
C(23)–N(5)–Li(2)	116.2(3)	C(32)–N(6)–C(28)	117.1(3)
C(32)–N(6)–Li(1)	118.3(3)	C(28)–N(6)–Li(1)	124.1(3)

Table 2 Selected bond lengths (Å) and angles (°) for **2**

Li(1)–N(5)	2.041(7)	Li(1)–N(6)	2.108(8)
Li(2)–N(5)	2.049(7)	Li(2)–N(6)	1.997(7)
Li(1)–N(1)	2.099(7)	Li(1)–N(2)	2.123(7)
Li(1)–N(3)	2.122(6)	Li(2)–N(4)	2.085(7)
N(1)–C(1)	1.341(5)	N(1)–C(5)	1.325(5)
N(2)–C(7)	1.329(5)	N(2)–C(11)	1.334(5)
N(3)–C(13)	1.341(5)	N(3)–C(17)	1.323(5)
N(4)–C(19)	1.331(5)	N(4)–C(23)	1.342(5)
N(5)–C(25)	1.363(5)	N(6)–C(31)	1.356(5)
N(5)–Li(1)–N(1)	119.3(3)	N(5)–Li(1)–N(6)	100.9(3)
N(1)–Li(1)–N(6)	121.1(3)	N(5)–Li(1)–N(2)	108.6(3)
N(1)–Li(1)–N(2)	101.6(3)	N(6)–Li(1)–N(2)	104.1(3)
N(6)–Li(2)–N(5)	104.6(3)	N(6)–Li(2)–N(4)	117.4(3)
N(5)–Li(2)–N(4)	118.9(3)	N(6)–Li(2)–N(3)	104.1(3)
N(5)–Li(2)–N(3)	112.9(3)	N(4)–Li(2)–N(3)	98.2(3)
C(5)–N(1)–C(1)	115.3(4)	C(5)–N(1)–Li(1)	116.3(3)
C(1)–N(1)–Li(1)	128.0(3)	C(7)–N(2)–C(11)	116.1(3)
C(7)–N(2)–Li(1)	129.3(3)	C(11)–N(2)–Li(1)	114.3(3)
C(17)–N(3)–C(13)	115.0(3)	C(17)–N(3)–Li(2)	111.2(3)
C(13)–N(3)–Li(2)	133.8(3)	C(19)–N(4)–C(23)	116.1(3)
C(19)–N(4)–Li(2)	121.1(3)	C(23)–N(4)–Li(2)	119.6(3)
C(25)–N(5)–Li(1)	127.1(3)	C(25)–N(5)–Li(2)	114.2(3)
Li(1)–N(5)–Li(2)	77.2(3)	C(31)–N(6)–Li(2)	131.2(3)
C(31)–N(6)–Li(1)	107.7(3)	Li(2)–N(6)–Li(1)	76.9(3)

[{PhN(H)Li·(4-Me-pyr)$_2$}$_2$] (**2**) and [{PhN(H)Li}$_4$·(4-Bu^t-pyr)$_6$] (**3**). A standard lithiation approach (eqn. (1)) was executed in

$$\text{Bu}^n\text{Li} + \text{PhNH}_2 \xrightarrow[-\text{Bu}^n\text{H}]{} [\text{PhN(H)Li}] \xrightarrow{4\text{-R-C}_5\text{H}_4\text{N}}$$

$$[\{\text{PhN(H)Li}\}_x\cdot(4\text{-R-C}_5\text{H}_4\text{N})_y] \quad (1)$$

each case, giving initially a precipitate of pure (solvent free) lithium anilide, which was subsequently treated with two molar equivalents of the chosen pyridine solvent.

The bulk solvents employed in these reactions were hexane–toluene mixtures of various proportions. In the cases of **1** and **2**, the two molar equivalents of coordinating solvent were needed to effect complete dissolution of the lithium anilide precipitate, consonant with the 1 : 2, lithium : pyridine solvent ratios found later in the isolated products. Toluene of crystallisation [one molecule per two (NLi)$_2$ dimers] was also present in the crystals of **2** used for the X-ray diffraction study. Whilst **3** was originally prepared in an analogous manner using the same 1 : 2 reaction stoichiometry, conducting a second experiment using the alternative stoichiometry found in the crystal (*i.e.*, 2 : 3) failed to bring about complete dissolution. Repeating the reaction with a greater excess of 4-*tert*-butylpyridine (4 molar equivalents per Li) and heating the resulting solution to reflux for 24 h still produced crystals of the solvent-limited tetranuclear structure **3** (see below). Thus, while **3** appears to be the only isolable product, its modest yield (best, 38%) combined with the mismatch between the crystal stoichiometry and the reaction stoichiometry indicates that most of the lithium anilide remains in solution, probably in the form of a higher solvated complex which is more soluble than **3**. From molecular models, a tetrasolvated dimer akin to **1** or **2** (see below) would seem to be a reasonable prospect for such from stereochemical considerations. The solubility of this hypothetical dimer would, in comparison to that of **1** or **2**, be augmented by the presence of the bulky *tert*-butyl substituent. The higher yields of isolated **1** and **2** (44% and 59% respectively) compared to that of **3** is therefore to be expected, though it is significant that they too fall well short of being quantitative.

Molecular structures

All three new lithium anilide solvates have been structurally characterised by X-ray diffraction studies. Since both are dimeric, the structures of **1** and **2** will be considered together

Table 3 Selected bond lengths (Å) and angles (°) for **3**

Li(1)–N(3)	2.091(5)	Li(1)–N(4)	1.983(5)
Li(2)–N(3)	2.627(5)	Li(2)–N(4)	2.013(4)
Li(2)–N(5)	2.005(5)	Li(2)–N(5A)	2.036(5)
Li(1)–N(1)	2.069(5)	Li(1)–N(2)	2.058(5)
N(1)–C(1)	1.317(3)	N(1)–C(5)	1.322(4)
N(2)–C(10)	1.339(3)	N(2)–C(14)	1.340(3)
N(3)–C(19)	1.344(3)	N(3)–C(23)	1.331(3)
N(4)–C(28)	1.378(3)	N(5)–C(34)	1.363(3)
N(4)–Li(1)–N(2)	127.3(2)	N(4)–Li(1)–N(1)	110.8(2)
N(2)–Li(1)–N(1)	105.8(2)	N(4)–Li(1)–N(3)	101.9(2)
N(2)–Li(1)–N(3)	103.8(2)	N(1)–Li(1)–N(3)	104.8(2)
N(5)–Li(2)–N(4)	128.1(3)	N(5)–Li(2)–N(5A)	103.1(2)
N(4)–Li(2)–N(5A)	121.2(2)	N(5)–Li(2)–N(3)	118.8(2)
N(4)–Li(2)–N(3)	84.93(17)	N(5A)–Li(2)–N(3)	95.0(2)
C(1)–N(1)–C(5)	115.5(2)	C(1)–N(1)–Li(1)	113.3(2)
C(5)–N(1)–Li(1)	131.1(2)	C(10)–N(2)–C(14)	114.9(2)
C(10)–N(2)–Li(1)	118.7(2)	C(14)–N(2)–Li(1)	124.1(2)
C(23)–N(3)–C(19)	115.5(2)	C(23)–N(3)–Li(1)	130.8(2)
C(19)–N(3)–Li(1)	113.4(2)	C(23)–N(3)–Li(2)	101.22(19)
C(19)–N(3)–Li(2)	103.8(2)	Li(1)–N(3)–Li(2)	71.46(17)
C(28)–N(4)–Li(1)	123.0(2)	C(28)–N(4)–Li(2)	127.0(2)
Li(1)–N(4)–Li(2)	88.5(2)	C(34)–N(5)–Li(2)	133.2(2)
C(34)–N(5)–Li(2A)	117.3(2)	Li(2)–N(5)–Li(2A)	76.9(2)

Symmetry transformations used to generate equivalent atoms: A: $-x + 1$, $-y + 1$, $-z$.

and first, before that of **3** which is tetranuclear. Selected dimensions for each complex are given in Tables 1–3.

Of the two dimers, **1** (Fig. 1) has the most familiar appearance as it exhibits a transoid arrangement of amido substituents with respect to the planar (NLi)$_2$ cyclic core (*i.e.*, its N–H bonds occupy opposite sides of this plane). In **2** (Fig. 2) a cisoid conformation is preferred, but the (NLi)$_2$ ring remains planar (sum of endocyclic bond angles, 359.6°, *cf.* 359.8° for **1**). Each structure is completed by terminally attached (two per Li centre) solvent ligands (pyr in **1**: 4-Me-pyr in **2**). The only other dimeric, unsubstituted anilide of lithium [{PhN(H)-Li·(THF)$_2$}$_2$], **4**, adopts a transoid arrangement as does its pentafluorinated analogue [{C$_6$F$_5$N(H)Li·(THF)$_2$}$_2$], **5**.[12] In the report of **4**,[12] considerable significance was placed upon the asymmetric bridging of lithium by the anilido N centres (N–Li bond lengths, 1.989 and 2.087 Å; difference, 0.098 Å), which was interpreted as a combination of N(sp^2)–Li and N(p)–Li bonds respectively within the centrosymmetric (NLi)$_2$ ring. This was accompanied by a small Li–N–(*ipso*)C–αC torsion angle of
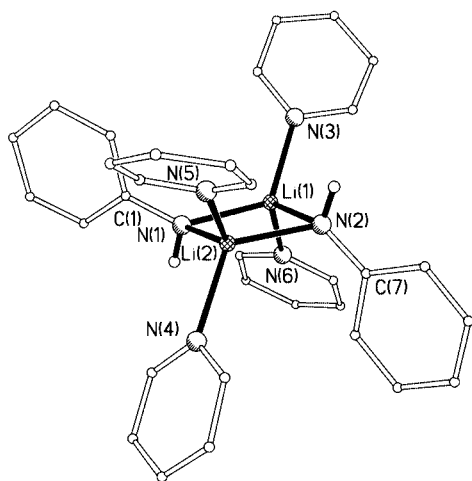
Fig. 1 Molecular structure of **1** showing the principal atom labels. Hydrogen atoms of N(H) bonds are included; others are omitted for clarity.
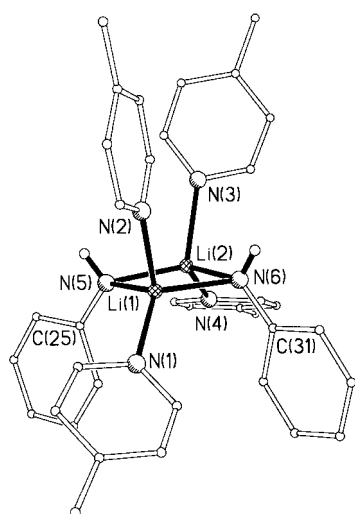

Fig. 2 Molecular structure of **2** showing the principal atom labels. Hydrogen atoms of N(H) bonds are included; others are omitted for clarity.

14.3°, indicating the near coplanarity of the N–Li bond with the anilide ligand plane. Furthermore a short N–(ipso)C bond length of 1.365 Å hinted at a π interaction between the aromatic system and the nitrogen p orbital. Comparison with **1** reveals a contrasting picture. As the structure is not crystallographically centrosymmetric, there are four distinct (anilido) N–Li bond lengths of 2.005(6), 2.018(7), 2.016(7) and 2.046(7) Å (mean, 2.021 Å; largest difference, 0.041 Å). Its corresponding torsion angles are substantially larger [e.g., Li(1)–N(1)–C(1)–C(6), −61.0(6)°; Li(1)–N(1)–C(1)–C(2), 118.7(5)°; Li(1)–N(2)–C(7)–C(8), −38.1(6)°; Li(1)–N(2)–C(7)–C(12), 144.4(4)°], signalling a greater twisting of the anilido planes with respect to the (anilido)N–Li bonds. Such significant geometrical distinctions are unlikely to be due exclusively to the different stereochemical profiles of THF and pyridine, especially as the latter molecule is planar and actually extends further away from the [(anilido)-N–Li]$_2$ core [i.e., mean (THF)O–Li bond length in **4**, 1.983 Å; mean (pyr)N–Li bond length in **1**, 2.084 Å]. When **2** is included in the comparison the bonding picture becomes even more complicated as the localized geometries surrounding its N anions more closely resembles those in **4** than in **1**. Non-centrosymmetric, the (NLi)$_2$ ring in **2** displays four unique bond lengths [1.997(7), 2.041(7), 2.049(7) and 2.108(8) Å] spanning a range of 0.111 Å. The Li(2)–N(6)–C(31)–C(32) torsion angle is exceptionally small at −11.0(6)°. Added to this, the geometry about N(6) involving atoms C(31)/H(6N)/Li(2) is essentially

planar (sum of bond angles, 357.2°), on discounting the exceedingly long N(6)–Li(1) bond [2.108(8) Å]. Note that in this analysis H(6N) was refined isotropically as was its (non-crystallographic) symmetrical counterpart H(5N). Thus, following the interpretation used previously to describe the bonding in **4**, the short N(6)–Li(2) [1.997(7) Å] and long N(6)–Li(1) bonds can be regarded as involving a N sp^2 orbital and a N p orbital respectively. However the second amide ligand of **2** does not fit so well into this bonding model. The major discrepancy concerns the symmetrical bridging to the Li centres which results in bond lengths equivalent within standard deviations [i.e., N(5)–Li(1), 2.041(7); N(5)–Li(2), 2.049(7) Å]. Whilst small, the torsion angle Li(1)–N(5)–C(25)–C(30) [−22.0(6)°] is twice that of the corresponding one involving N(6). Disregarding the N(5)–Li(2) bond, there is also a modest reduction in the sum of bond angles around N(5) (353.3°), in comparison with that around N(6), though it too approaches planarity. However, no distinction can be drawn between the two unique (anilido)N–(ipso)C bond lengths [N(5)–C(25), 1.363(5); N(6)–C(31), 1.356(5) Å], which are of a similar length to the short one in **4** (1.365 Å). Hence the second pair of N–Li bonds in **2** involving N(5) can, using a similar interpretation, be considered to have more sp^3 character than those involving N(6). The origin of these subtle but significant geometrical distinctions among the structures of **1**, **2** and **4** is clearly a complex matter involving an interplay of steric and electronic factors. Whether it is reasonable to describe them in terms of a localised bonding model invoking hybridisation is open to question anyway, given the highly polar nature of the N$^{δ-}$–Li$^{δ+}$ bonds of the anilide, which is amplified in the presence of donor solvent ligands. That notwithstanding, it is unequivocal that the anionic N centres in these dimers can adopt flexible geometries spanning the extremes of tetrahedral and trigonal pyramidal (or trigonal bipyramidal with one vacant axial site) coordination. Furthermore the [(anilido)N–Li]$_2$ rings can take up either transoid (anti) or cisoid (syn) conformations. Intuitively, one would expect the former conformation, where the larger phenyl substituents reside on opposite sides of the [(anilido)N–Li]$_2$ plane, to be more thermodynamically stable; however, it is likely that the energy differential involved is relatively minor such that small changes in the stereochemistry and/or electronic makeup of the solvent ligand could tip the balance in favour of the latter conformation. The direction of approach and site of attack of the solvent ligand towards uncomplexed lithium anilide (presumably a long oligomeric ladder, though its precise structure has not yet been definitely established) could also influence the choice of conformation particularly as a lithium primary amide polymeric ladder [{[PhCH$_2$N(H)Li]$_2$·THF}$_∞$][10] with alternating, contiguous transoid and cisoid (NLi)$_2$ rings has recently been crystallographically characterised. Entropic considerations may also drive the choice of conformation. In this regard, it is pertinent to note that the dimeric primary amidogallane [{Me$_2$Ga[μ-N(H)Bu^t]}$_2$][14] undergoes a transoid–cisoid isomerisation in solution at 80 °C as determined by a time-resolved ^{1}H NMR study: the transoid isomer is thermodynamically preferred, but a positive ΔS during the isomerisation process favours the cisoid isomer. This increase in entropy was attributed to the lower symmetry of the latter. The rhodium(I) anilide complex [{(Ph$_3$P)$_2$Rh-[μ-N(H)Ph]}$_2$][15] is also thought to exist as a mixture of transoid and cisoid conformers.

Turning to the structure of **3** (Fig. 3), in the context of the preceding discussion of **1** and **2**, the most easily identifiable fragment of this more complicated assembly is its central, dimeric [(anilido)N–Li]$_2$ ring. The imposed symmetry of this centrosymmetric structure dictates a transoid arrangement for this ring, which is also strictly planar. Through the spiro-atoms Li(2) and Li(2A), a tricyclic system is formed (Fig. 4), the outer (N–Li)$_2$ rings of which are distinctly non-planar (sum of endo-cyclic bond angles, 346.79°; RMS deviation from planarity,

Table 4 ¹H NMR chemical shifts (in ppm) for **1–3**[a]

	N(H)	*ortho*H	*meta*H	*para*H	αH	βH	γH	Me
1	3.17	6.67	7.08	6.48	8.37	6.62	6.96	—
2	3.21	6.74	7.15	6.52[b]	8.36	6.52	—	1.77
3	3.14	6.66	7.10	6.53	8.37	6.77	—	0.94

[a] Recorded in [²H₈]-toluene solutions at 300 K. [b] Obscured by the βH resonance.
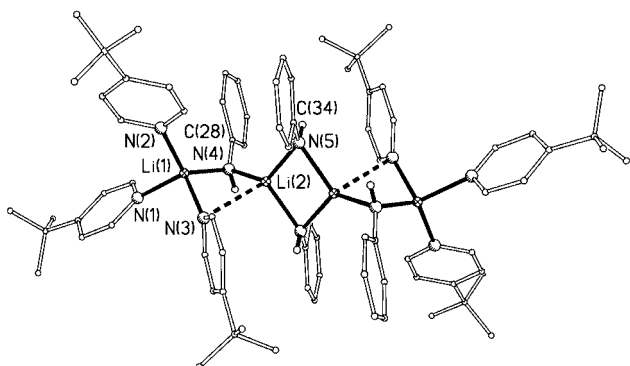
Fig. 3 Molecular structure of **3** showing the principal atom labels. Hydrogen atoms of N(H) bonds are included; others are omitted for clarity.
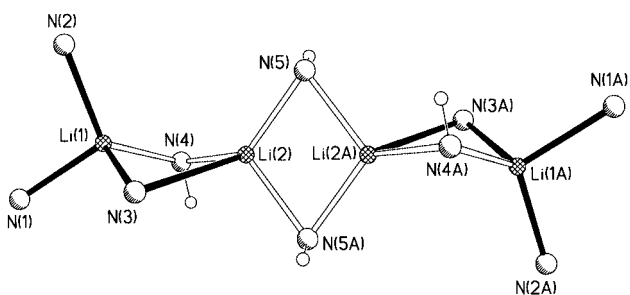
Fig. 4 View highlighting the tricyclic inorganic core of **3**.

0.247 Å). In a further distinction, the μ-N atoms in the outer rings belong to different ligands: N(4) is part of an anionic anilide; while N(3) is part of a neutral 4-Bu^t-pyr molecule. It is rare for a neutral or alkyl-substituted pyridine to bridge metal centres. To the best of our knowledge it has not been observed previously with lithium in a crystal structure; however, it has been reported with other metals such as molybdenum in [(MoO)₂-(C₈H₉PS₂)₄(OS)₂·pyr] [16] and silver in [(AgI)₂{P(C₆H₁₁)₃}₂·pyr]. [17] The structure of **3** therefore contains two distinct types of Li atom, though both occupy distorted tetrahedral geometries (mean bond angle: Li1, 109.1°; Li2, 108.5°). Three anilido N atoms and one substituted-pyridine N atom surround Li2 in the central ring, while one anilido N atom and three substituted-pyridine N atoms surround Li1 in the outer ring. The more asymmetrical coordination about the transoid (N–Li)₂ ring in **3** compared to that in **1** has little effect on bond lengths (mean, 2.021 and 2.025 Å respectively), or on endocyclic bond angles [at N, 76.9(2)° and (mean) 76.7° respectively; at Li, 103.1(2)° and (mean) 103.2° respectively]. Also the geometry at N(5) in **3** more closely approaches distorted tetrahedral than distorted trigonal pyramidal as gauged by relevant torsion angles [*e.g.*, Li(2)–N(5)–C(34)–C(39), 58.8(4)°; Li(2)–N(5)–C(34)–C(35), −119.5(3)°; Li(2A)–N(5)–C(34)–C(39), −37.7(12)°; Li(2A)–N(5)–C(34)–C(35), 141.9(9)°] and the sum of bond angles around N(5) involving the C(34), H(5N), and Li(2) atoms (342.0°) [*i.e.*, excluding those involving the longer N(5)–Li(2A) bond]. Accordingly, from the perspective of these parameters the central (NLi)₂ ring fragment of **3** corresponds to a conventional transoid lithium amide dimer. However, the distinction is that the coordination of Li(2) is completed by another anilide anion through N(4) [bond length, 2.013(4) Å] and one

solvent ligand through N(3), instead of by the more usual two solvent ligands (or one didentate type). There is a precedent for a trianilide–lithium coordination in the structure of the aforementioned [{PhN(H)Li}₃·2PMDETA], [13] though significantly the lithium atom involved is only three coordinate overall [mean N–Li bond length, 1.984 Å, *cf.* 2.018 Å for the three (anilido)N–Li(2) bonds in **3**]. In contrast, **3** displays an additional fourth coordination between Li(2) and N(3) (marked by a broken line in Fig. 3), which belongs to the unique bridging 4-Bu^t-pyr ligand. The great length of this contact [2.627(5) Å] coupled with the near-orthogonal dihedral angle it makes with the pyridine ring plane (114.0°), suggests it is primarily a weak π interaction involving a p orbital on N. By similar reasoning, the N(3)–Li(1) bond, which is substantially shorter [2.091(5) Å] and is inclined almost linear to the pyridine ring plane (dihedral angle, 170.0°), can be considered as a stronger σ interaction involving the *exo* sp² orbital of N. Comparison with the series of halide structures solvated by the same alkylpyridine [LiX·(4-Bu^t-pyr)₃] [18] (where X = Cl, Br, or I) reveals N–Li bond lengths of a similar magnitude (range, 2.03–2.11 Å; mean, 2.06 Å) to the latter type in **3**. The bonds between each terminally attached solvent ligand and Li(1) in **3** are also of a comparable length (mean, 2.064 Å). Completing the coordination of Li(1) is N(4), the only anionic centre bound to this cation. Consequently, this represents the shortest (anilido)N–Li bond in the structure [length, 1.983(5) Å]. The mixed bridge nature of the outer Li(2)N(3)Li(1)N(4) rings leads to large deviations in the endocyclic bond angles (*i.e.*, 16.97° between the NLiN ones and 17.04° between the LiNLi ones). There is also a significant widening of the intra-solvent ligand bond angle N(1)Li(1)N(2) [105.8(2)°] in comparison to the corresponding one in the unsubstituted-pyridine solvate **1** (mean value, 100.0°). While this reflects the steric influence of the additional *tert*-butyl substituent in **3**, it must be borne in mind that the ring environments of the affected Li atoms are not identical.

NMR spectroscopic studies

The three new lithium anilide solvates have also been characterised by ¹H, ⁷Li and ¹³C NMR spectroscopic studies in [²H₈]-toluene solution. In each case the spectra recorded at room temperature are consistent with the empirical formula of the solvate as established by the X-ray crystallographic study. Table 4 compares the ¹H chemical shifts for **1–3**. Here the similarity of the data obtained for the individual anilide anions suggests that their electronic environments (or more precisely, their time-averaged ones) are nearly equivalent, despite each compound having a unique solvating ligand. It is discernible that the anilide anion chemical shifts for **2** are generally at higher frequencies than those for **1** and **3**, but the margin of difference does not appear significant. There is also little difference between the chemical shifts of corresponding hydrogen atoms on the pyridine and substituted-pyridine ligands. As the resonance of the *para*H atom on the anilide ring of **2** is obscured by that of the βH atom on the 4-Me-pyr ring, the spectrum was re-recorded in [²H₆]-benzene solution: this established distinct, separate resonances at 6.55 and 6.41 ppm respectively. Though not listed in Table 4, the toluene of crystallisation in **2** detected in the crystal structure is also present in the ¹H NMR spectra. Table 5 compares the ¹³C chemical shifts for **1–3**. Again corresponding resonances for the anilide anions appear at near-equivalent

Table 5 ^{13}C NMR chemical shifts (in ppm) for **1**–**3**[a]

	*ipso*C	*ortho*C	*meta*C	*para*C	αC	βC	γC	CH$_3$	C(CH$_3$)$_3$
1	161.4	116.3	129.7	111.4	150.2	125.5	135.5	—	—
2	161.5	116.3	129.8	111.5	150.0	124.5	146.4	20.5	—
3	159.8	116.7	130.2	112.9	150.6	121.1	160.3	30.6	34.8

[a] Recorded in [²H₈]-toluene solutions at 300 K.
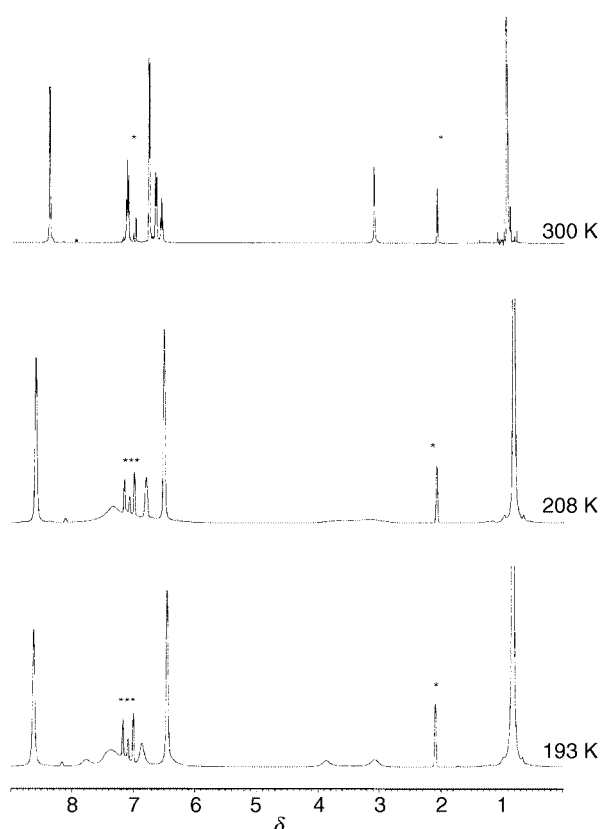
Fig. 5 Variable-temperature ^{1}H NMR spectra of **3** in [²H₈]-toluene solution. The asterisks represent signals due to solvent.

positions. As expected the only major distinction concerns the γC resonances of the pyridine solvent ligands which move sequentially to higher frequency (by 10.9 and 13.9 ppm increments, respectively) as the attached substituent changes in the order H to Me to Bu^t. This trend of similar chemical shifts for corresponding atoms continues in the room temperature ^{7}Li NMR spectra of **1**, **2** and **3**, which all exhibit a single resonance (at 3.36, 3.47 and 3.45 ppm, respectively). From this it could be interpreted that each Li atom experiences a similar coordination environment (under conditions which favour fast exchange processes). This reasoning is consistent with the common distorted tetrahedral geometry found for the Li atoms in the crystal structures. However, since the crystal structure of **3** displays two distinct types of Li atom (in contrast to the solitary type observed in **1** and **2**), it was of interest to examine its solution characteristics further by performing variable-temperature experiments. Accordingly, ^{7}Li NMR spectra in [²H₈]-toluene solution were recorded in the range 300–193 K. While its position (relative to that of LiCl in D$_2$O at 0.00 ppm) moves progressively to a higher frequency on lowering the temperature (4.04 ppm at 193 K), a single resonance is observed throughout. Among the possible scenarios that could explain this observation are (i) the crystal structure is not retained in solution, but a new structure with a single type of Li atom is formed; (ii) the crystal structure is retained in solution, but its two distinct types of Li atom have identical chemical shifts (an example of accidental equivalence); or (iii) the crystal structure is retained in solution, but its two distinct types of Li atom

are exchanging rapidly in a process with a low energy barrier. Recorded over the same temperature range (300–193 K), the ^{1}H NMR spectra prove to be more informative. Fig. 5 shows these spectra at three key temperatures (300, 208 and 193 K). At the coldest temperature (which favours slow exchange) two N(*H*) resonances are clearly evident (at 3.86 and 3.07 ppm) in a 1:1 population ratio. Coalescence of these two resonances occurs at 208 ± 2 K. On warming the solution further there now exists a single N(H) resonance which sharpens gradually as the temperature is increased. Closer inspection of this set of spectra reveals that the *ortho*H resonance of the anilido anion undergoes an analogous process: there is one sharp signal at 300 K (at 6.66 ppm), which broadens and decoalesces at intermediate temperatures (at 208 K, it lies underneath the *meta*H and [²H₈]-toluene solvent arene signals), and two separate signals at 193 K (one at 7.76 ppm; the other is obscured by the βH signal). Note that in contrast there is only one *meta*H and one *para*H anilide signal over the same temperature range (though both are broad at 193 K), which presumably reflects their distant positioning from the ligating N centre. Furthermore the coalescence phenomena were found to be independent of the concentration of the solution. Thus it can be concluded that there are two distinct types of anilide anion present in a 1:1 molar ratio which appear equivalent on the NMR timescale at 300 K. This observation is consistent with the crystal structure, where there are bridging anilide anions [at N(5)] and, discounting the long π-based bond between N(3) and Li(2), 'terminal' ones [at N(4)] with respect to the Li(2)N(5)Li(2A)N(5A) ring. Therefore, the dynamic process observed in solution can be tentatively assigned to the intramolecular exchange of these bridging and 'terminal' anilide ligands.

Experimental

Syntheses and characterisation

Reactions were performed in Schlenk tubes under a protective atmosphere of dry, oxygen-free, argon. *n*-Butyllithium was purchased from Aldrich and re-standardised before each application, using the diphenylacetic acid reagent-indicator method.[19] Aniline was triply distilled, deoxygenated by the freeze–pump–thaw method,[20] and dried over molecular sieves before being employed in a reaction. Though this procedure was found to significantly slow down the formation of the oxidation product aniline black, it could not be completely eradicated. Pyridine was triply distilled, stored over molecular sieves, and freeze–pump–thawed to remove traces of oxygen prior to use. 4-Methylpyridine and 4-*tert*-butylpyridine were purchased from Lancaster and dried over molecular sieves before being employed in a reaction.

NMR spectral data were recorded on a Bruker DPX 400 spectrometer operating at 400.13 MHz for ^{1}H, 100.62 MHz for ^{13}C, and 155.50 MHz for [7]Li. Chemical shifts are quoted relative to TMS at 0.00 ppm (for ^{1}H and ^{13}C) and to LiCl in D$_2$O at 0.00 ppm (for [7]Li). ^{13}C NMR assignments were verified by HMQC experiments.

Solvate 1. A solution of Bu^{n}Li (10 mmol) in hexane was reduced *in vacuo* to leave a colourless oily residue, which was subsequently treated with toluene (5 ml). Aniline (10 mmol) was then added to the chilled solution to obtain a white precipi-

Table 6 Crystallographic data

Compound	1	2·0.5C₇H₈	3
Formula	$C_{32}H_{32}Li_2N_6$	$C_{36}H_{40}Li_2N_6 \cdot 0.5C_7H_8$	$C_{78}H_{102}Li_4N_{10}$
M	514.5	616.7	1207.5
Crystal system	Orthorhombic	Monoclinic	Triclinic
Space group	$Pna2_1$	$C2/c$	$P\bar{1}$
$a/\text{Å}$	18.104(3)	42.397(6)	12.0898(18)
$b/\text{Å}$	11.5602(16)	9.614(2)	12.1766(18)
$c/\text{Å}$	14.2505(19)	18.024(4)	13.717(2)
$a/°$			106.324(3)
$\beta/°$		98.287(6)	101.859(3)
$\gamma/°$			98.673(4)
$U/\text{Å}^3$	2982.4(8)	7270(3)	1849.2(5)
Z	4	8	1
$D_c/\text{g cm}^{-3}$	1.146	1.130	1.084
μ/mm^{-1}	0.07	0.07	0.06
Reflections measured	12310	20565	11139
Unique reflections	4291	6394	6298
R_{int}	0.0340	0.0597	0.0436
No. of refined parameters	368	407	430
wR (F^2, all data)	0.1594	0.2258	0.1719
R (F, $F^2 > 2\sigma$)	0.0604 (3767)	0.0790 (4016)	0.0629 (3595)
Max., min. electron density/e Å^{-3}	0.72, −0.28	0.23, −0.26	0.29, −0.27

tate of lithium anilide as butane gas was evolved. 20 mmol of pyridine were then required to achieve complete dissolution. Cooling of the resulting pale yellow solution to *ca.* −7 °C afforded colourless crystals of **1** (1.13 g, 44%), mp 102–104 °C (Found: C, 73.9; H, 6.0; N, 15.3; Li, 2.5. $C_{16}H_{16}N_3Li$ requires C, 74.7; H, 6.2; N, 16.4; Li, 2.7%). ¹H NMR (400.13 MHz in [²H₈]-toluene, 300 K) δ 8.37 (d, 4H, αH-pyr), 7.08 (t, 2H, *meta*H-Ph), 6.96 (t, 2H, γH-pyr), 6.67 (d, 2H, *ortho*H-Ph), 6.62 (t, 4H, βH-pyr), 6.48 (t, 1H, *para*H-Ph) and 3.17 (s, 1H, NH). ⁷Li NMR (155.50 MHz in [²H₈]-toluene, 300 K) δ 3.36 (s). ¹³C NMR (100.62 MHz in [²H₈]-toluene, 300 K) δ 161.4 (*ipso*C-Ph), 150.2 (αC-pyr), 135.5 (γC-pyr), 129.7 (*meta*C-pyr), 125.5 (βC-pyr), 116.3 (*ortho*C-Ph) and 111.4 (*para*C-Ph).

Solvate 2. A solution of BuⁿLi (5 mmol) in hexane was chilled in an ice bath. Aniline (5 mmol) was added dropwise to this solution, resulting in the formation of a white precipitate of lithium anilide as butane gas was evolved. The precipitate was broken up into a fine dispersion by immersing the solution in an ultrasonic bath for a few minutes. Two molar equivalents (10 mmol) of 4-Me-pyr were then added to produce, on heating, an orange homogeneous solution. Turning cloudy on cooling, the mixture was subsequently treated with toluene (1 ml) and re-heated. Cooling the resulting solution to *ca.* −30 °C for two days afforded colourless crystals of **2**·0.5 toluene (0.92 g, 59%), mp 60 °C (Found: C, 76.9; H, 8.4; N, 13.1; Li, 2.4. $C_{36}H_{40}N_6$-$Li_2 \cdot 0.5C_7H_8$ requires C, 76.9; H, 7.1; N, 13.6; Li, 2.3%). ¹H NMR (400.13 MHz in [²H₈]-toluene, 300 K) δ 8.36 (d, 4H, αH-pyr), 7.15 (t, 2H, *meta*H-Ph), 6.74 (d, 2H, *ortho*H-Ph), 6.52 (m, 5H, overlapping *para*H-Ph and βH-pyr), 3.21 (s, 1H, NH) and 1.77 (s, 6H, CH₃-pyr). ¹H NMR (400.13 MHz in [²H₆]-benzene, 300 K) δ 8.32 (m, 4H, αH-pyr), 7.10 (t, 2H, *meta*H-Ph), 6.75 (d, 2H, *ortho*H-Ph), 6.55 (t, 1H, *para*H-Ph), 6.41 (m, 4H, βH-pyr), 3.23 (s, 1H, NH) and 1.62 (s, 6H, CH₃-pyr). Note that toluene of crystallisation was also present in both ¹H NMR spectra. ⁷Li NMR (155.50 MHz in [²H₈]-toluene, 300 K) δ 3.47 (s). ¹³C NMR (100.62 MHz in [²H₈]-toluene, 300 K) δ 161.5 (*ipso*C-Ph), 150.0 (αC-pyr), 146.4 (γC-pyr), 129.8 (*meta*C-Ph), 124.5 (βC-pyr), 116.3 (*ortho*C-Ph), 111.5 (*para*C-Ph) and 20.5 (CH₃-pyr).

Solvate 3. Lithium anilide (5 mmol) was prepared as a suspension in hexane as in the procedure for **1** and **2** above. Two molar equivalents (10 mmol) of 4-Buᵗ-pyr were added drop-wise to this chilled mixture to produce, on heating, a yellow transparent solution. This turned turbid on cooling to room

temperature. Therefore, toluene (2 ml) was introduced and the mixture was re-heated until a homogeneous solution was reformed. Standing this solution at ambient temperature for ten days afforded a crop of colourless crystals of **3** (0.57 g, 38%), mp 77–80 °C (Found: C, 77.6; H, 8.7; N, 10.0; Li, 2.2. $C_{19.5}H_{25.5}N_{2.5}Li$ requires C, 77.6; H, 8.5; N, 11.6; Li, 2.3%). ¹H NMR (400.13 MHz in [²H₈]-toluene, 300 K) δ 8.37 (m, 4H, αH-pyr), 7.10 (t, 2H, *meta*H-Ph), 6.77 (m, 4H, βH-pyr), 6.66 (d, 2H, *ortho*H-Ph), 6.53 (t, 1H, *para*H-Ph), 3.14 (s, 1H, NH) and 0.94 (s, 9H, (CH₃)₃C). (193 K) 8.63 (αH-pyr), 7.76 (*ortho*H-Ph), 7.36 (*meta*H-Ph), 6.86 (*para*H-Ph), 6.45 (overlapping *ortho*H-Ph and βH-pyr), 3.86 (NH), 3.07 (NH) and 0.82 ((CH₃)₃C). ⁷Li NMR (155.50 MHz in [²H₈]-toluene, 300 K) δ 3.45 (s). (193 K) 4.04 (s). ¹³C NMR (100.62 MHz in [²H₈]-toluene, 300 K) δ 160.3 (γC-pyr), 159.8 (*ipso*C-Ph), 150.6 (αC-pyr), 130.2 (*meta*C-Ph), 121.1 (βC-pyr), 116.7 (*ortho*C-Ph), 112.9 (*para*C-Ph), 34.8 ((CH₃)₃C) and 30.6 (CH₃).

Crystal structure determination

Crystals of the three compounds were examined on a Bruker AXS SMART CCD diffractometer at 160 K, with Mo-Kα radiation ($\lambda = 0.71073$ Å). Selected crystallographic data are in Table 6. Methods were as described previously.[21] Hydrogen atoms were refined with a riding model to maintain expected geometry, except for free refinement of those attached to nitrogen atoms; N–H bond lengths were restrained to 0.90 Å in compound **1**.

CCDC reference number 186/1872.

See http://www.rsc.org/suppdata/dt/b0/b000576m/ for crystallographic files in .cif format.

References

1 M. F. Lappert, P. P. Power, A. R. Sanger and R. C. Srivastava, *Metal and Metalloid Amides*, Ellis Horwood Limited, Chichester, 1980; L. Brandsma and H. D. Verkruijsse, *Preparative Polar Organometallic Chemistry*, Springer, Berlin, 1987, vol. 1; B. J. Wakefield, *Organolithium Methods*, Academic Press, London, 1987; M. Fieser, *Reagents for Organic Synthesis*, Interscience, New York, 1990, vol. 15; P. R. Jenkins, *Organometallic Reagents in Synthesis*, Oxford University Press, Oxford, 1992.

2   A. G. Myers, T. Yoon and J. L. Gleason, *Tetrahedron Lett.*, 1995, **36**, 4555.

3   R. E. Allan, M. A. Beswick, N. Feeder, M. Kranz, M. E. G. Mosquera, P. R. Raithby, A. E. H. Wheatley and D. S. Wright, *Inorg. Chem.*, 1998, **37**, 2602.

4   F. M. Mackenzie, R. E. Mulvey, W. Clegg and L. Horsburgh, *J. Am. Chem. Soc.*, 1996, **118**, 4721. See also, R. Holland, J. C. Jeffery and C. A. Russell, *J. Chem. Soc., Dalton Trans.*, 1999, 3331.

5   R. Fleischer, S. Freitag, F. Pauer and D. Stalke, *Angew. Chem.*, 1996, **108**, 208; *Angew. Chem., Int. Ed. Engl.*, 1996, **35**, 204.

6   K. Gregory, P. v. R. Schleyer and R. Snaith, *Adv. Inorg. Chem.*, 1991, **37**, 47; R. E. Mulvey, *Chem. Soc. Rev.*, 1991, **20**, 167.

7   G. R. Kowach, C. J. Warren, R. C. Haushalter and F. J. DiSalvo, *Inorg. Chem.*, 1998, **37**, 156.

8   A. R. Kennedy, R. E. Mulvey and A. Robertson, *Chem. Commun.*, 1998, 89.

9   R. E. Mulvey, *Chem. Soc. Rev.*, 1998, **27**, 339.

10 W. Clegg, S. T. Liddle, R. E. Mulvey and A. Robertson, *Chem. Commun.*, 1999, 511.

11 W. Clegg, L. Horsburgh, F. M. Mackenzie and R. E. Mulvey, *J. Chem. Soc., Chem. Commun.*, 1995, 2011.

12 R. v. Bülow, H. Gornitzka, T. Kottke and D. Stalke, *Chem. Commun.*, 1996, 1639.

13 D. Barr, W. Clegg, L. Cowton, L. Horsburgh, F. M. Mackenzie and R. E. Mulvey, *J. Chem. Soc., Chem. Commun.*, 1995, 891. For an example of a sodium substituted-anilide PMDETA complex, see I. Cragg-Hine, M. G. Davidson, A. J. Edwards, P. R. Raithby and R. Snaith, *J. Chem. Soc., Dalton Trans.*, 1994, 2901.

14 J. T. Park, Y. Kim, J. Kim, K. Kim and Y. Kim, *Organometallics*, 1992, **11**, 3320.

15 J.-J. Brunet, G. Commenges, D. Neibecker, K. Philippot and L. Rosenberg, *Inorg. Chem.*, 1994, **33**, 6373.

16 M. G. B. Drew, P. C. H. Mitchell and A. R. Read, *J. Chem. Soc., Chem. Commun.*, 1982, 238.

17 G. A. Bowmaker, Effendy, P. J. Harvey, P. C. Healy, B. W. Skelton and A. H. White, *J. Chem. Soc., Dalton Trans.*, 1996, 2459.

18 C. L. Raston, B. W. Skelton, C. R. Whitaker and A. H. White, *Aust. J. Chem.*, 1988, **41**, 341.

19 W. G. Kofron and L. M. Baclawski, *J. Org. Chem.*, 1976, **41**, 1879.

20 R. J. Errington, *Advanced Practical Inorganic and Metalorganic Chemistry*, Blackie Academic and Professional, London, 1997, p. 82.

21 C. Redshaw, V. C. Gibson, W. Clegg, A. J. Edwards and B. Miles, *J. Chem. Soc., Dalton Trans.*, 1997, 3343.

Paper b000576m